

Thermomigration produced by collision cascades in solid solutions

E. Lopasso, M. Caro, and A. Caro

Centro Atómico Bariloche, 8400 Bariloche, Argentina

(Received 2 March 2000; revised manuscript received 13 October 2000; published 4 April 2001)

Using the molecular dynamics of a model system, we determine the role of thermomigration, one of the thermodynamic forces that may affect the mass transport under the extreme conditions of time, temperature, and length scales characteristics of a heat spike following a collision cascade. By studying heat spikes in liquid alloys, we are able to isolate the Soret effect and measure the magnitude of the heat of transport Q^* . We find that this effect can give rise to an increase or a decrease of solute content in the core of a cascade. We show the particular case of the Au-Ni system (complete solubility in the high-temperature solid phase and above), in which Ni as a solute in Au has a tendency to move toward the hot core of the spike. The opposite is true for Au as a solute in Ni. This effect appears in a system whose initial condition before irradiation is the equilibrium thermodynamic phase predicted by the phase diagram, and therefore no solute motion is expected.

DOI: 10.1103/PhysRevB.63.174105

PACS number(s): 61.80.Az, 66.30.-h, 82.20.Wt

The effects of energetic-particle irradiation on pure elements and alloys have received significant attention for decades, and, in particular with the progress of computational physics, numerical simulations have contributed substantially to our understanding of these complex phenomena.¹ The modification of the microstructure following such events is of both technological and scientific interest in fields like ion implantation and nuclear technology, and in general for all material processes far from equilibrium.

Two stages in the collision event can clearly be identified: ballistic and thermal. In the first stage the kinetic energy of the atoms involved in the event is above the threshold for displacement; interstitial atoms are created far from the center of the cascade through mechanisms like replacement collision sequences, while vacancies are left close to it. Rapidly, the total energy evolves toward a situation close to equipartition between kinetic and potential energies, indicating the beginning of the thermal phase; then the core of the cascade behaves as a liquid. Ion mixing results in both stages. Finally, a temperature drop drives the system toward resolidification. In most materials explored, these stages last a few psec. The annealing phase follows the cascade, and involves diffusion in the solid phase. For a review of this subject, see Ref. 2.

In the case of alloys, the processes mentioned above may drive the target either toward or away from equilibrium microstructures. In fact, irradiation induces precipitation as well as dissolution in both saturated and nonsaturated solid solutions, and many other possible transformations like amorphization, order-disorder, etc. Part of the complexity comes from the competition between opposite effects: the enhanced atomic mobility—due to the increased defect concentration and temperature—affects the kinetics of precipitation or ordering, which in turn are oppositely affected by disordering and precipitate dissolution produced by mixing. For a review of a theoretical thermodynamic description of materials under such driving conditions, see Ref. 3.

A simple question that still remains without a precise quantitative answer is the role of thermodynamic forces during the thermal phase of a cascade. In other words, given an arbitrary dilute alloy, what would be the effect of ion beam

irradiation at low temperature, where the mobility of the irradiation-created point defects is small? Would zones affected by cascades be richer or poorer in solute? (We note here that we address the problem of the thermal phase alone.) Such an elementary question is still open, and is difficult to answer in quantitative terms.

From the point of view of computer simulations, attention was recently focused on the thermodynamics of collision cascades in alloys. Intrinsic limitations in the theoretical models used for the atomic interactions restrict the number of systems that can reliably be described. The heat of solution between some transition metals, solubility limits, ordered phases, and some intermetallics can be included in the models. In this way, several aspects have been studied: collision cascades in ordered intermetallics, for example, induce changes (disordering, amorphization) that are controlled by factors including the kinetics of disordering in the liquid core and the short-range order of the liquid.⁴ Also, cascades in an interface between immiscible materials are much less efficient at inducing ion mixing.^{5,6} The research subject is rich because the energetic particles induce ultrafast nanoscale phase transitions in situations where thermodynamic variables like thermal gradients, quenching rates, and pressures are quite different from the usual laboratory conditions.

At least four different regimes are expected to contribute to the evolution of the microstructure of a binary mixture under ion irradiation. (i) In the ballistic stage, different cross sections for the different species may lead to differences in the amount of mass transport between solute and solvent. (ii) In the early stages of the heat spike, when the core of the cascade is liquid, thermomigration induced by the huge thermal gradient may induce solute transport; this is the Soret effect.⁷ Also, immiscibility in the liquid phase may induce decomposition of nonequilibrium solutions. (iii) In the resolidification phase, it is known that for pure elements the solid-liquid interface pushes the vacancies toward the liquid phase, producing an inverse flux of atoms;^{8,9} however, another possible contribution is the crossing of a two phase field delimited by the solidus-liquidus lines which induces compositional changes. Finally, (iv) In the solid phase, the

quenched core of the cascade may have a composition different from the equilibrium, and solid-state diffusion will drive the solute toward it.

Points (i) and (iv) received significant attention, but here we focus our attention on the second regime: the liquid phase of the cascade. Most binary liquid alloys of segregating transition metals are single-phase homogeneous solutions characterized by some short-range chemical order, like Co-Cu, Ag-Cu, and Fe-Cu. Few cases, however, in which the heat of mixing is large and positive, lead to a heterogeneous liquid phase like Ni-Ag. Therefore, if the unirradiated initial condition of a segregating alloy is a nonequilibrium homogeneous solid phase (for a concentration beyond the solubility limit), a relevant question is what the effect of a collision cascade will be. Several recent papers address this issue.¹⁰⁻¹³ For the case of a heterogeneous liquid the cascade will probably induce segregation, while for homogeneous liquids the question is subtler.

In this paper we address an issue that is not related to the heat of mixing. By performing computer simulations of thermomigration and heat spikes in equilibrium Au-Ni solid solutions, a model system with complete solubility, we determine the influence of the Soret effect in the thermal phase of a collision cascade as a source of solute migration in systems under irradiation. To isolate this effect from points (i), (iii) and (iv) of above, we produce the heat spike on a liquid sample, where no vacancies or solid-liquid interfaces appear. Also, no collisional mixing and no multiphase equilibrium states appear.

The interest in such thermodynamic effects in binary systems is the natural continuation of numerous works in computer simulations of radiation effects.¹⁰⁻¹³ In particular, in a previous work we analyzed this problem in combination with a rigorous treatment of the Stefan problem.¹⁴

In a dilute, high-temperature, liquid solution of B and A under a thermal gradient, the solute flux is approximately given by (the exact expression contains the gradient of the chemical potential instead that of the concentration, but for the conditions considered here this approximation is adequate)

$$\mathbf{J}_B = -D \left(\nabla c_B + \frac{Q^* c_B}{kT^2} \nabla T \right), \quad (1)$$

where \mathbf{J}_B is the flux of solute (B) particles, $D = D_0 \times \exp(-H_m/kT)$ is the solute diffusion coefficient, and c_B is its concentration; H_m is the migration enthalpy, k is the Boltzmann constant, and T the temperature. Q^* is the heat of transport, whose sign can be either positive or negative for different solute-solvent combinations and is the key parameter relating the generalized force (∇T) to the generalized displacement (\mathbf{J}_B) in the Onsager formalism of irreversible thermodynamics.^{15,7} Fick's second law holds for \mathbf{J}_B given by Eq. (1):

$$\frac{\partial c_B}{\partial t} = -\nabla \cdot \mathbf{J}_B. \quad (2)$$

Q^* is a physical constant characteristic of the system, independent of the heat of mixing. Besides the principles of linear irreversible thermodynamics that lead to Eq. (1), a simple picture in terms of jump frequencies provides a partial interpretation for the second term in the right-hand side of Eq. (1). The driving force for thermomigration can be divided into an intrinsic portion and a portion coupled to the heat carriers: electrons and phonons. The intrinsic considerations include the energy transported by the moving particle and the energy required to prepare a place to receive it, the Wirtz model.^{16,17} In this way, the migration enthalpy H_m splits into βH_m and αH_m , with $\beta + \alpha = 1$. βH_m is the fraction of the enthalpy of diffusion that is required by the moving atom at $x - \Delta x$ to reach the saddle point configuration at x , while αH_m is the fraction required for the atoms that are located close to the saddle point. With these arguments, the jump rate from left to right in a thermal gradient is

$$\Gamma_{L \rightarrow R} = \nu_0 \exp\{-[\beta H_m/kT_{x-\Delta x}] - [\alpha H_m/kT_x]\}. \quad (3)$$

Consideration of the rate in the opposite direction gives a net flow

$$J = c(x)[\Gamma_{L \rightarrow R} - \Gamma_{R \rightarrow L}] = (D/kT)c(x)\beta H_m \nabla T/T, \quad (4)$$

with the implication that the heat of transport Q^* is equal to βH_m . This picture, of course, allows a unique sign for Q^* , and relates it to a fraction of the migration enthalpy. For some systems this approximation is satisfactory, with $\beta \sim 0.8$. However, consideration of the other driving forces results in contributions that may even give a change of Q^* 's sign.¹⁸ The heat flux is given by an equation similar to Eq. (1), with the same two generalized forces, implying that the solutions for temperature and solute concentration as a function of time and position from a system of two coupled differential equations.

Our goal is to analyze this effect under the conditions of a heat spike produced by a collision cascade, to determine whether it may play a role in some particular systems. To this end, we first fit the results of computer simulations of a

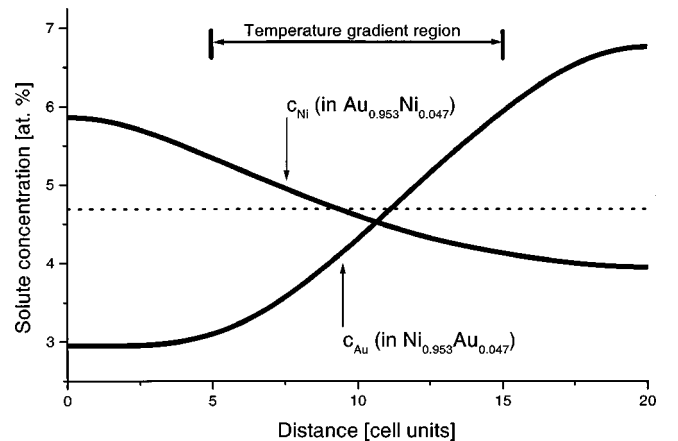


FIG. 1. Stationary solute concentration after 500 psec in a uniform thermal gradient for both systems studied: $\text{Ni}_{0.953}\text{Au}_{0.047}$ and $\text{Au}_{0.953}\text{Ni}_{0.047}$. In both cases, the dashed lines correspond to a concentration without a thermal gradient.

TABLE I. Values of the activation enthalpy and pre-exponential factor for diffusion of both solute and solvent in the systems studied. The last row shows the heat of transport for both solutes.

	Ni in $\text{Ni}_{0.953}\text{Au}_{0.047}$	Au in $\text{Ni}_{0.953}\text{Au}_{0.047}$	Ni in $\text{Au}_{0.953}\text{Ni}_{0.047}$	Au in $\text{Au}_{0.953}\text{Ni}_{0.047}$
D_0 ($\text{\AA}^2/\text{psec}$)	7.1 ± 0.7	6.4 ± 0.7	9.1 ± 4.3	8.3 ± 2.4
H_m (eV)	0.54 ± 0.03	0.52 ± 0.03	0.49 ± 0.16	0.50 ± 0.01
Q^* (eV)		0.48	-0.24	

very simple case, namely, a linear stationary thermal gradient, to the numerical solutions of Eqs. (1) and (2), to determine both the validity of these equations and the value of Q^* . We then use this value of Q^* to predict the magnitude of the modifications in the solute concentration as a result of thermomigration in a thermal spike; finally, this prediction will be compared to the actual simulation of a spike. To focus only on thermomigration, eliminating other thermodynamic forces such as those coming from the two-phase field between the solidus and liquidus lines, we consider the particular case of a heat spike in a liquid mixture. In this way, the only possible source of an eventual concentration gradient is thermomigration; therefore, with this kind of computer experiment we are able to isolate this and determine its magnitude.

The molecular-dynamics (MD) simulations were done on the Au-Ni system because it shows complete solubility in the solid phase, different melting points, large liquidus-solidus splitting (for a future determination of its influence in solute motion), and good embedded-atom-model (EAM) potentials for the interactions.¹⁹ These potentials reliably predict the main features of the equilibrium phase diagram, in particular the heats of mixing, which are 0.3 eV/Au atom in Ni-Au (the experimental value is 0.28 eV/atom) and 0.08 eV/Ni atom in Au-Ni (the experimental value is 0.22 eV/atom). We model fcc lattices of $\text{Au}_{0.953}\text{Ni}_{0.047}$ and $\text{Ni}_{0.953}\text{Au}_{0.047}$ with $40 \times 8 \times 8$ cubic cells of dimension a_0 and periodic boundary conditions, with their crystalline axis aligned along the Cartesian coordinates. The concentration value 4.7% comes from replacing, at random, six out of 128 atoms of solvent by a solute in each of the $\{200\}$ planes of the structure. The samples are first equilibrated at 3000 K and zero pressure; this determines the a_0 's used as normalized length units. Then a thermal gradient is applied in the x direction by turning on a thermostat at temperature T_L in the ten external layers (five cells) at the $+x$ and $-x$ boundaries of the sample, and another thermostat at T_H acting on the 20 central

layers. In this way, a gradient $\pm(T_H - T_L)/10a_0$ acts on ten cells at both sides of the samples, with the minus sign for the right side and the plus sign for the left. Two thermal gradients are explored, namely, with $T_L - T_H = 2000 - 5000$ K and $5000 - 15000$ K, respectively, the latter with the same sample volume corresponding to 3000 K at zero pressure. MD runs are then performed at a constant volume, simulating the extreme high pressure existing in an actual spike. The solute concentration is measured every 5 psec, and runs are 500 psec long. An adequate equilibration time allows a full relaxation of the pressure waves originating in the inhomogeneous thermal expansion.

Figure 1 shows stationary concentration profiles for the large gradient case, averaged over the two halves of the samples and smoothed by smearing out the x coordinate of each atom by a Gaussian of width $2a_0$, as a function of distance to the center. Cell units are used in the x axis to report both alloys on the same scale [$a_{0\text{Ni}}(3000\text{K}) = 3.93 \text{\AA}$ and $a_{0\text{Au}}(3000\text{K}) = 4.41 \text{\AA}$ for the Ni- and Au-rich cases, respectively]. Due to the large temperature variations and the corresponding thermal expansion, the samples have inhomogeneous density. Curves in Fig. 1 represent the solute concentration in at. % which are obtained as the ratio between the solute density (in atoms/ \AA^3) over the sample density. They indicate an evident Soret effect. The curve for Ni, in $\text{Au}_{0.953}\text{Ni}_{0.047}$, shows an increased value at the high-temperature end of the sample, and evidence of a negative Q^* , while the complementary system $\text{Ni}_{0.953}\text{Au}_{0.047}$ shows the opposite behavior. This figure shows that in the range of thermal gradients and length scales appearing in the thermal phase of collision cascades, thermomigration contributions to the modification of solute distribution are to be expected in a system that otherwise has no reasons to show such behavior.

From Eq. (1), with $J_{\text{Ni,Au}} = 0$, the concentration in the stationary state follows the expression $\ln(c_{\text{Ni,Au}}) = Q_{\text{Ni,Au}}^*/kT + C$, that could be used to determine Q^* without knowing

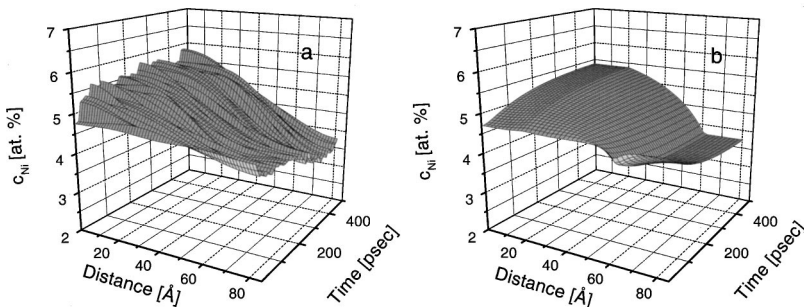


FIG. 2. Ni concentration in $\text{Au}_{0.953}\text{Ni}_{0.047}$ measured in the MD simulation of the static thermal gradient (left), and calculated with Eqs. (1) and (2) (right).

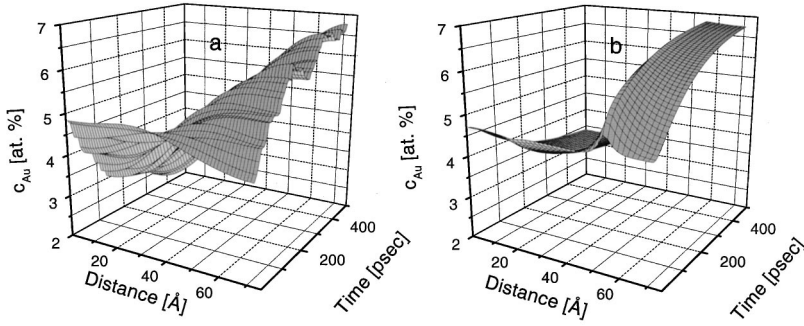


FIG. 3. Au concentration in $\text{Ni}_{0.953}\text{Au}_{0.047}$ measured in the MD simulation of the static thermal gradient (a), and calculated with Eqs. (1) and (2) (b).

the diffusion coefficient; however, to improve the precision of the fitting procedure and explore the time dependence, we use the whole time-space evolution $c(x,t)$. For this purpose, the diffusion coefficients of Au and Ni in both Ni-Au liquid solutions is first determined by MD simulations in the temperature range and concentration of interest. The results for D_0 and H_m from measurements of the mean-square displacement as a function of time and temperature are still well represented by an Arrhenius law, despite the significant thermal expansion appearing in this temperature range (17%).

It is important to point out that the EAM potentials used in this work were designed to describe several properties of the solid phase. Its use for liquid alloys at elevated temperatures is an extrapolation that is by no means intended to predict quantitative values, but to highlight physical effects in a model system. We determine the diffusion coefficient in both alloys between 2000 and 4000 K at constant zero pressure, and then explore the pressure dependence. 4000 K appears to be below the boiling point in both cases for these potentials, while experimental melting temperatures are around 3000 K. Results are reported in Table I. As expected, the migration enthalpies of solute and solvent are very similar in both alloys, reflecting similarities in the interatomic potentials, as implied from the complete solubility in the solid phases. Pre-exponential factors, on the other hand, show a ratio in the right direction, but smaller than expected from the mass relation in an Einstein model, namely, $D_{0\text{Ni}}/D_{0\text{Au}} = (m_{\text{Au}}/m_{\text{Ni}})^{1/2} = 1.8$ versus -1.1 in the simulations in both alloys. As for the pressure dependence, we analyzed diffusion at 4000 K, with the volume corresponding to 3000 K and zero pressure. This is obtained by applying 35 kbar. The diffusion coefficients of the solute and solvent in $\text{Ni}_{0.953}\text{Au}_{0.047}$ decrease from 1.51 and 1.60 $\text{\AA}^2/\text{psec}$ to 1.16 and 1.30 $\text{\AA}^2/\text{psec}$, respectively. For simplicity this 20–30%

difference will be neglected in the numerical analysis that follows by assuming a constant diffusion coefficient, independent of pressure.

Table I also shows the values of Q^* (-0.24 eV for Ni and 0.48 eV for Au, both as solutes) determined by minimizing the sum of the absolute values of $c(x,t)$ obtained from the solutions of Eqs. (1) and (2) minus the values obtained in the MD simulations.

Figures 2 and 3 show the surfaces $c_{\text{Ni}}(x,t)$ in $\text{Au}_{0.953}\text{Ni}_{0.047}$ and $c_{\text{Au}}(x,t)$ in $\text{Ni}_{0.953}\text{Au}_{0.047}$, respectively. Parts (a) in these figures are the results of MD, and parts (b) are the predictions of Eqs. (1) and (2) with the parameters reported in Table I. The conclusion that clearly emerges at this point is that thermomigration plays a measurable role in the time, size, and temperature regimes characteristics of cascades. A significant concentration gradient appears, showing that Ni as solute in Au has a tendency to move toward the high-temperature side and, inversely, Au as solute in Ni moves toward the low- T end. Measured values for self-diffusion in Au in the solid phase (that is, vacancy thermomigration), the closest experimental value to compare with, gives -0.26 eV.²⁰

It is then natural to ask whether this effect, so far neglected in the analysis of impurity motion in collision cascades, may contribute to it in a measurable amount. This point is explored next by introducing a thermal spike in a liquid sample. In this way, collisional mixing, solidification interface, and vacancy motion are absent, leaving thermomigration as the sole possible source of solute motion.

For the simulations of thermal spikes, we use samples containing $100 \times 10 \times 10$ cells of a mixture with 4% solute, both Au in Ni and Ni in Au (eight atoms replaced by solute at random in every $\{200\}$ plane). The thermal spike is introduced in the center of the sample by assigning three-

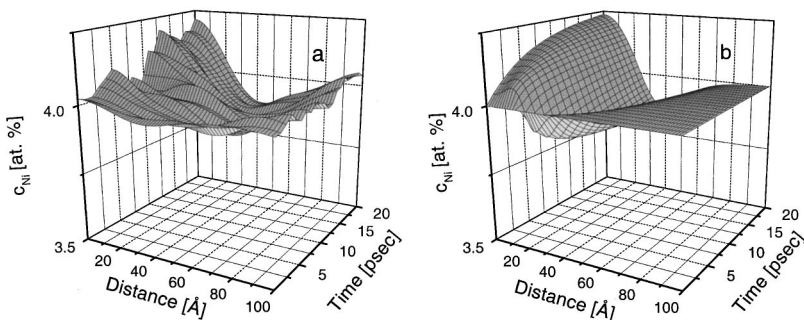


FIG. 4. Ni concentration in $\text{Au}_{0.95}\text{Ni}_{0.04}$ measured in the MD simulation of the heat spike (a) and calculated with Eqs. (1) and (2) (b).

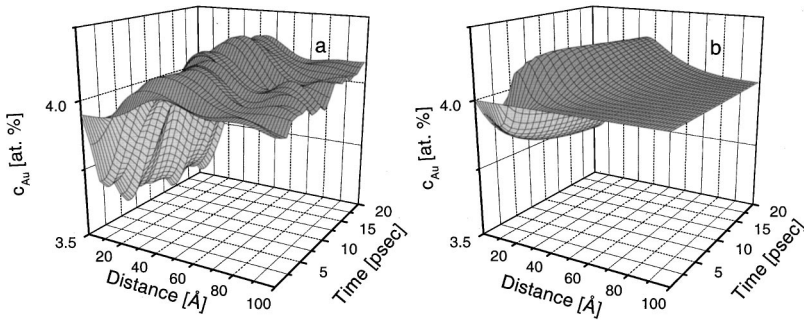


FIG. 5. Au concentration in $\text{Ni}_{0.96}\text{Au}_{0.04}$ measured in the MD simulation of the heat spike (a) and calculated with Eqs. (1) and (2) (b).

dimensional random velocities corresponding to a temperature profile following a one-dimensional Gaussian shape along the x direction, with dispersion equal to two cells, in a sample originally equilibrated at 2500 K. Ten layers at both extremes of the sample are kept at 2500 K, with a thermostat during the whole simulation. The initial central temperature of the spikes was in the range between 15 000 and 50 000 K, corresponding to energy densities comparable to those in cascades of some keV in these materials (~ 1 eV/atom). Simulations are done at constant volume. The surface $T(x,t)$ is obtained, and cuts $T(x,t_\alpha)$ at discrete set of times $\{t_\alpha\}$, are adjusted with Gaussians, which is equivalent to assume a constant thermal conductivity, an approximation that proved to be reasonably good. For details about a more precise determination of the thermal conductivity, see Ref. 8.

With this $T(x,t)$ as an input database, and the heat of transport measured previously, we are able to solve Eqs. (1) and (2) numerically for $c(x,t)$. This is shown for both alloys in parts (b) of Figs. 4 and 5. From the MD simulations of the spike we obtain another determination of $c(x,t)$, which is shown in parts (a) of these figures. These figures constitute the main contribution of this paper. They show that, in a system where no thermodynamic forces that originate in the equilibrium phase diagram justify any increase or decrease of solute atom concentration in the core of a cascade, a clear tendency toward such variations appears. The effect results from thermomigration in the liquid phase of the alloy, the Soret effect, whose magnitude and sign is determined by the heat of transport of the solute in the particular solvent. In the case of Au, with the largest Q^* , Fig. 5 shows a fluctuation larger than 10% between the concentration in the enriched part and the depleted part.

Although the Soret effect was first observed more than a century ago, to our knowledge this is the first time its effects are observed in a computer simulation of an ultrafast process at the nanoscale. Its quantitative description in terms of a linear approximation (valid for small gradients) seems to hold, as was also shown for thermal transport in heat spikes in Ref. 8, proving the adequacy of the linear irreversible thermodynamics approximation approach under such extreme conditions. It is important to point out that thermomigration is not related to the effect that the heat of solution has on solute transport in nonequilibrium situations. In fact for

the system under consideration here, the liquid phase used as an initial condition is a homogeneous solution at equilibrium; no segregation due to a positive heat of mixing is expected. In this sense, this work does not address the same issue as those treating mixing of bilayers in immiscible compounds,^{5,21} or decomposition of unstable alloys.⁶

In the MD simulation there are additional effects that are neglected in the analytic solution; in particular, heat transport is not the only means of energy extraction from the core of the spike; elastic waves originating in the sudden volume expansion carry out a fraction of the energy. Also, the finite size of the sample produces reflection back and forth of this wave in a cycle of about 4 psec, generating noise in the measured values. This, in part, justifies the noisy aspect of Figs. 4(a) and 5(a). The fact that the concentration appears as a quotient between two quantities, the measured atomic concentration of solute and the density of the sample, as discussed in the presentation of Fig. 1, also contributes to the noise in these figures. Nonetheless, the effect is clear, and points toward the interest in further studying the other thermodynamic forces mentioned above, as a way to derive predictive capabilities about the behavior of binary mixtures under high-energy particle irradiation.

In summary, using the molecular dynamics of a model system, we determine the role of thermomigration under the extreme conditions of time, temperature and space scales characteristics of a heat spike following a collision cascade. By studying heat spikes in liquid Au-Ni alloys, we are able to isolate the Soret effect and measure the magnitude of the heat of transport Q^* . We find that Ni as a solute in Au has a tendency to move toward the hot core of the spike, while the opposite is true for Au as a solute in Ni. This effect is not related to properties of the equilibrium phase diagram, such as the heat of mixing.

Preliminary results on the Fe-Cu system seem to indicate that Cu has a positive Q^* in Fe, showing a tendency to move away from the core, in opposition to the force derived from the free energy of the saturated solid solution, that tends to precipitate it. Competition between them therefore makes it possible to study this issue of wide interest.

This work was partially supported by Conicet PIP 4205/96, PIP 0664/98, and IAEA Research Contract No. 9253.

- ¹*Fundamentals of Radiation Damage*, edited by A. Dunlop, F. Rullier-Albenque, C. Jaouen, C. Templier, and J. Davenas [Solid State Phenom. **30-31** (1993)].
- ²R. S. Averback and T. Diaz de la Rubia, in *Solid State Physics*, edited by H. Ehrenreich and F. Spaepen (Academic, New York, 1998), Vol. 51, p. 281.
- ³G. Martin and P. Bellon, in *Solid State Physics*, edited by H. Ehrenreich and F. Spaepen (Academic, New York, 1996), Vol. 50, p. 189.
- ⁴M. Spaczer, A. Caro, and M. Victoria, Phys. Rev. B **52**, 7171 (1995).
- ⁵K. Nordlund, J. Keinonen, M. Ghaly, and R. S. Averback, Nucl. Instrum. Methods Phys. Res. B **165**, 441 (2000).
- ⁶T. J. Colla, H. M. Urbassek, and R. S. Averback, Nucl. Instrum. Methods Phys. Res. B **153**, 369 (1999).
- ⁷S. R. de Groot, in *Thermodynamics of Irreversible Processes* (North-Holland, Amsterdam, 1952).
- ⁸H. van Swygenhoven and A. Caro, Phys. Rev. Lett. **70**, 2098 (1993).
- ⁹K. Nordlund, M. Ghaly, R. S. Averback, M. Caturla, T. Diaz de la Rubia, and J. Tarus, Phys. Rev. B **57**, 7556 (1998).
- ¹⁰N. Soneda and T. Diaz de la Rubia, Philos. Mag. A **78**, 995 (1998).
- ¹¹K. Nordlund and R. S. Averback, Phys. Rev. B **59**, 20 (1999).
- ¹²A. Almazouzi, M. J. Caturla, M. Alurralde, T. D. de la Rubia, and M. Victoria, Nucl. Instrum. Methods Phys. Res. B **160**, 311 (2000).
- ¹³K. Nordlund, L. Wei, Y. Zhong, and R. S. Averback, Phys. Rev. B **57**, 13 965 (1998).
- ¹⁴A. Caro, M. Alurralde, R. Saliba, and M. Caro, J. Nucl. Mater. **251**, 72 (1997).
- ¹⁵L. Onsager, Phys. Rev. **38**, 2265 (1931).
- ¹⁶K. Wirtz and J. W. Hibi, Phys. Z. **44**, 369 (1943).
- ¹⁷L. A. Girifalco, Phys. Rev. **128**, 2630 (1962).
- ¹⁸Paul Shewmon, *Diffusion in Solids* (Mineral, Metals & Materials Society, Warrendale, PA, 1989).
- ¹⁹S. M. Foiles, M. I. Baskes, and M. S. Daw, Phys. Rev. B **33**, 7983 (1986).
- ²⁰H. B. Huntington, in *Diffusion*, edited by H. I. Aaronson (American Society for Metals, Metals Park, OH, 1973), Chap. 6, p. 155.
- ²¹H. M. Urbassek and H. Gades, Nucl. Instrum. Methods Phys. Res. B **115**, 485 (1996).